

1 **MINERALOGICAL AND CHEMICAL CHARACTERIZATION**
2 **OF LUNAR HIGHLAND SOILS:**
3 **INSIGHTS INTO THE SPACE WEATHERING**
4 **OF SOILS ON AIRLESS BODIES**

5
6 **Lawrence A. Taylor¹, Carlé Pieters²,**
7 **Allan Patchen¹, Dong-Hwa S. Taylor¹,**
8 **Richard V. Morris³, Lindsay P. Keller³, and David S. McKay³**

9
10 **¹ Planetary Geosciences Institute**
11 **Dept. of Earth & Planetary Sciences**
12 **University of Tennessee**
13 **Knoxville, TN 37996,(lataylor@utk.edu)**

14
15 **² Dept. of Geological Sciences**
16 **Brown University**
17 **Providence, RI 02912**

18
19 **³ Code KR**
20 **NASA/Johnson Space Center**
21 **Houston, TX 77058.**

22
23 **SUBMITTED TO: Journal Of Geophysical Research**

24 **CONTACT: Larry Taylor**

25 **REVISED: 9 August 2009**

26 **Abstract.** With reflectance spectroscopy, one is measuring only properties of the fine-grained
27 regolith, most affected by space weathering. The Lunar Soil Characterization Consortium has
28 undertaken the task of coordinated characterization of lunar soils, with respect to their mineralog-
29 ical and chemical makeup. It is these lunar soils that are being used as “ground-truth” for all air-
30 less bodies. Modal abundances and chemistries of minerals and glasses in the finest size frac-
31 tions (20-45, 10-20, and <10 μm) of four Apollo 14 and six Apollo 16 highland soils have been
32 determined, as well as their bulk chemistry and I_S/FeO values. Bi-directional reflectance mea-
33 surements (0.3–2.6 μm) of all samples were performed in the RELAB. A significant fraction of
34 nanophase Fe^0 (np- Fe^0) appears to reside in agglutinitic glasses. However, as grain size of a soil
35 decreases, the percentage of total iron present as np- Fe^0 increases significantly, whereas the ag-
36 glutinitic glass content rises only slightly; this is evidence for a large contribution to the I_S/FeO
37 values from the surface-correlated nanophase Fe^0 , particularly in the <10 μm size fraction. The
38 compositions of the agglutinitic glasses in these fine fractions of the highland soils are different
39 from the bulk-chemistry of that size; however, compositional trends of the glasses are not the
40 same as those observed for mare soils. It is apparent that the glasses in the highland soils contain
41 chemical components from outside their terrains. It is proposed that the Apollo 16 soils have
42 been adulterated by the addition of impact-transported soil components from surrounding maria.

43

44

45 **1. Introduction**

46 The varied processes of space weathering that occur during soil formation on the Moon are
47 thought to be similar to those for many other airless bodies (e.g., Phobos, Eros, Mercury) al-
48 though different in magnitude and cumulative effect. Therefore, the study of these effects within
49 lunar soils should form the basis for our understanding of the regoliths on other heavenly bodies.
50 This is a particularly applicable axiom for reflectance spectroscopy of these soils. It has been
51 repeatedly demonstrated that it is the fine fractions (<45 μm) that dominate the spectral reflec-
52 tance signatures of lunar soils [Pieters, 1983, 1993; Pieters et al., 1993; Hapke, 2001]. The 10-20
53 μm size fraction is the most similar to the overall spectral properties of the bulk soil. However, it
54 is also the finer-size fractions that concentrate the major products of space weathering, e.g., na-
55 nophase metallic iron (np- Fe^0), that affect the overall continuum and strength of absorption fea-

56 tures of the observed spectra.

57 Using the Apollo and Luna lunar soils to document the products of space weathering, we
58 have studied a selected suite of the Apollo 14 and 16 highland soils (**Table 1**). This study is a
59 continuation to our characterization of the mineralogical and glassy components of the fine frac-
60 tions of lunar mare soils [e.g., Taylor et al., 2001a, b; Pieters et al., 2000, 2001], especially the
61 complicated agglutinitic glass [Basu et al., 1996; Basu and Molinaroli, 2001;]. Specific soils
62 were chosen for their representation of diverse degrees of maturation. These Apollo highland
63 soils may represent a large portion of the nearside of the Moon. Many systematics of the pro-
64 gression of soil properties with decreasing grain size are similar to those of mare soils, which ap-
65 peared to support the Fusion-of-the-Finest Fraction model [Papike et al., 1982] for lunar soil
66 formation. However, the relationships of the bulk composition of the size fractions for the Apol-
67 lo 14 and 16 soils to that of the composition of agglutinitic glass are quite different from those
68 for mare soils and appear to be in an opposite sense. This may necessitate modifications to the
69 soil formation paradigm, and was first addressed by Pieters and Taylor [2003a].

70 **1.1. Lunar Soil Characterization Consortium**

71 In order to document the space weathering effects on lunar spectra, the Lunar Soil Characte-
72 rization Consortium (LSCC) was established [Taylor et al., 1999; 2001b] for the collaborative
73 study of lunar soils. This group of lunar soil scientists brings different expertise and instrumental
74 techniques related to the quantification of space-weathering effects and the deciphering of these
75 effects in reflectance spectra. The members of this LSC Consortium are D.S. McKay {size sepa-
76 ration}, R.V. Morris {FMR}, L.P. Keller {TEM/SEM}, C.M. Pieters {Spectral Reflectance}, and
77 L.A. Taylor {bulk chemistry; modal characterization/mineral chemistry}.

78 **1.2. Suite of Lunar Highland Soils**

79 In a logical continuation of our soil characterization studies for mare soils, we have selected a
80 suite of lunar highland soils to represent the diversity in soil maturities, using the concept of
81 I_{q}/FeO values from Morris [1976]. These soils are listed in Table 1. “Pristine” samples of each
82 of them were allocated by the Curation and Planning Team for Extra-Terrestrial Materials
83 (CAPTEM), and the curatorial staff at Johnson Space Center efficiently handled the necessary
84 allocations. The actual sample handling logistics and allocations are presented in Figure 1 of

85 Taylor et al. [2001a].

86 **2. Methodology**

87 **2.1. Size Separation**

88 Four Apollo 14 and six Apollo 16 highland soils were sieved in the laboratory of D.S.
89 McKay at Johnson Space Center. Triply-distilled water was used through out the process. At
90 first, the lunar sample allocation of the <1 mm size portion of each pristine soil was sieved to ob-
91 tain a <45 μm size fraction. A split of this <45 μm fraction was then sieved into the three size
92 ranges: 20-45 μm , 10-20 μm , and <10 μm . Great care was taken to assure the size fractions retain
93 their natural soil properties, especially grain coatings. According to the same distribution plan as
94 utilized for the mare soils [Taylor et al., 2001b], samples of each of the size splits were taken and
95 distributed to members of the LSCC for their specific analysis.

96 **2.2. Bulk-Sample Chemical Analyses**

97 Major-element chemistry was determined on portions of each size fraction. The fused-
98 bead technique was used for preparation of the samples for electron microprobe analyses. In a
99 stream of dry nitrogen gas, approximately 5 mg of representative sample was fused on a Mo-strip
100 heater. The samples were heated to a melt, held for 20-30 sec, and quenched by rapidly reducing
101 the heat input (i.e., turning off the current). The resulting glasses were mounted in a multi-holed
102 plastic disk, impregnated with epoxy, polished, coated with carbon, and subjected to at least 10
103 electron microprobe analyses per glass, using a 20 μm beam size, 15 Kv potential, and 20 nA
104 beam current on the Cameca SX-50 EMP at the University of Tennessee.

105 **2.3. Modal Analyses by Electron Microprobe**

106 Detailed petrographic properties of lunar highland soils, particularly the finer fractions, are
107 poorly known. With these fine-grain sizes (i.e., <45 μm), normal optical-microscopic techniques,
108 that are typically used are not efficient. Therefore, modern techniques are required to character-
109 ize soil compositions and mineral modes with the accuracy and precision needed for spectroscop-
110 ic modeling. The polished grain mounts prepared by the Curatorial Staff at Johnson Space Cen-
111 ter formed the basis for all modal and phase characterization. Using the technique presented by
112 Taylor et al. [1996], accurate modal analyses were performed with an Oxford Instrument Energy

113 Dispersive Spectrometer Unit (EDS) on a Cameca SX-50 electron microprobe at the University
114 of Tennessee. Through use of Oxford Instruments *FeatureScan* software, it was possible to rea-
115 dily determine the modal proportions of minerals and glasses in thousands of fine particles in the
116 20-45 μm , 10-20 μm , and $<10 \mu\text{m}$ size fractions of the lunar soils. This is based upon gathering
117 energy dispersive (EDS) chemical data from 150,000-200,000 points on the phases (not epoxy)
118 in each grain mount, thereby classifying the minerals by their chemistry. Additional programs
119 allowed for the determination of the average chemical composition of each mineral and glass
120 phase. The phase compositional data, as well as all our soil characterization data for both the
121 mare and the highland soils studied by the LSCC are accessible at
122 <http://web.utk.edu/~pgi/data.html>.

123 **2.4. Difficulties in Modal Analyses of Minerals and Glasses in Highland Soils**

124 The first studies of the LSCC were performed with mare soils [Taylor et al., 2001a, b], and
125 mare soils were chosen to start our characterization because they contain minerals and glasses
126 that have vastly contrasting chemistries – e.g., pyroxene versus plagioclase versus agglutinitic
127 glass – thereby making their identification by chemistry relatively easy. It was anticipated that
128 applications of our mare-based, X-ray digital-imaging analysis scheme to highland soils would be
129 considerably more difficult and time-consuming than for the mare soils. This is largely due to
130 the limited compositional range of highland soils, each with a bulk composition that approx-
131 imates plagioclase feldspar with only minor mafic components (e.g., ~5 wt% FeO). These sever-
132 al considerations needed to be made in order to make more effective the application of our tech-
133 niques to highland soils.

134 The composition of the minerals and glasses in the three size fractions of the four Apollo 14
135 and six Apollo 16 soils (Table 1) were determined by the extensive analyses of each phase. The
136 agglutinitic glass was especially placed in close scrutiny. Inasmuch as the composition of the ag-
137 glutinitic glass in highland soils is not far removed from that of the highland bulk soil, and the
138 bulk soil is near that of pure plagioclase, this glass closely mimics plagioclase. Therefore, expe-
139 riments were conducted with the electron microprobe and the EDS unit in order to consider the
140 several key parameters that determine the precision of the EDS X-ray analyses [Taylor et al.,
141 2001c; 2002; 2003]. For example, it was been observed that 20 kV excitation is better than the

142 15 kV typically used by most EMP users [Taylor et al., 1996].

143 For the highland soils, a digital map of the entire section of the grain mount is first made,
144 and many agglutinates, displaying vesicular texture, as well as other phases, are optically identi-
145 fied by reflected light microscopy. The initial examination with the EMP consists of wave-
146 length-dispersive spectral (WDS) EMP determinations of the compositional limits of all the opti-
147 cally identified minerals and glasses from direct analyses of ~1000-3000 phases, in particular the
148 agglutinitic glasses. With a given soil, it is necessary to perform such initial characterization, for
149 even subtle differences in chemistry can change the “chemical windows” for a mineral or glass.
150 In particular, the agglutinitic glasses are all alumina-rich, but the agglutinitic glass, and the minor
151 amount of non-agglutinitic impact glass, can be distinguished from plagioclase (including maske-
152 lynite) by their FeO and MgO contents. As demonstrated by McGee [1993], all lunar highland
153 plagioclase contains <0.5 wt% FeO and <0.5 wt% MgO. We verified this for the identified ag-
154 glutinitic and impact glasses. These glasses then formed the compositional basis for our EDS
155 modal analyses.

156 In this study, non-agglutinitic, impact-produced glasses are also reported as agglutinitic glass,
157 since the compositions from our analyses appear similar and because most of the impact-
158 produced glasses in the fine-grain sizes examined in this study contain np-Fe⁰. In the modal val-
159 ues for agglutinitic glass, we estimate that the other non-agglutinitic, impact glasses usually con-
160 sist of <10% of the glass present. There is no doubt that some small amount of “non-agglutinitic
161 (i.e., impact) glasses” might have been included, particularly in the finest grain size.

162 **2.5. Ferromagnetic Resonance (FMR) Analyses**

163 The detection and analyses of the abundances of single-domain np-Fe⁰ were determined by
164 Ferromagnetic Resonance (FMR) measurements performed in the Magnetism Lab of R.V. Mor-
165 ris, at Johnson Space Center. It has been in this laboratory that virtually all the FMR measure-
166 ments on lunar samples have been made since 1972, ensuring consistency, accuracy, and preci-
167 sion.

168 **3. Modal Analyses of Minerals and Glasses**

169 The modal abundances of 12 different minerals and glasses were determined on polished

170 grain mounts of each of the 30 size splits (10 soils X 3 sizes). This was performed utilizing the
171 X-ray digital imaging technique outlined by Taylor et al. [1996], with several modifications de-
172 tailed above. The modal data for the major phases in the Apollo 14 and 16 soils are given in Ta-
173 ble 2 and graphically shown in Figure 1. The pyroxene values are for total pyroxene, calculated
174 by combining abundances of the four (4) different pyroxene compositions that were determined.
175 The actual breakdown of these total-pyroxene abundances is given in Table 3. It should be no-
176 ticed that a designation has been made for a “K-phase”, which is for the “KREEPY” phases (e.g.,
177 K-rich feldspar; K-rich glasses) typically associated with the Apollo 14 soils. The compositions
178 of the minerals and agglutinitic glass in the size fractions of these Apollo soil are given in Table
179 4.

180 As shown by comparison of different soils in Figure 1, there is an overall increase in the ab-
181 undance of agglutinitic glass as the soils mature, from low to high I_S/FeO values. This correlates
182 with the general decrease in the amounts of the minerals and is to be expected, since the longer
183 the exposure of soil on the surface of the Moon, the greater the effects of micro-meteorite gar-
184 dening and general space weathering (Taylor and McKay, 1992). This extended presence at the
185 lunar surface results in an increase in the melted products (i.e., agglutinates, agglutinitic glass,
186 and vapor-deposited patinas), due to the impacting processes.

187 Within a given soil, a similar scheme is apparent from larger to finer size fractions. With
188 decrease in grain size, the abundances of the agglutinitic glasses increase (with the exception of
189 the $<10\ \mu\text{m}$ fraction of 14141-5.7). Although there is also a tendency for the plagioclase to
190 slightly increase in the finer fractions, there are distinct decreases in pyroxene and olivine with
191 decreasing grain size. Therefore, the ferro-magnesian minerals decrease proportionately, while
192 the plagioclase abundances stay constant or increase slightly. These trends are also apparent with
193 the bulk chemistry of the various size fractions, as presented below.

194 The designation of ilmenite in the modes includes minor amounts of Ti-Cr-rich spinels
195 ($<1\%$). Although low in abundance (i.e., $<2\%$), ilmenite in the Apollo 14 soils, in particular,
196 shows a general slight increase with decreasing grain size (Table 2), contrary to that in mare soils
197 [Taylor et al., 2001a, b]. These observations for the Apollo 14 and 16 soils, some of which were
198 also seen with the mare soils, are addressed by Pieters and Taylor [Pieters and Taylor, 2002,
199 2003a, b].

200

201 **4. Soil Chemistry**

202 Several systematic changes can be readily observed in Figure 2 and Table 4 with respect to
203 the bulk chemistry of each of the size fractions of the highland soils. The composition of a lunar
204 highland soil systematically changes as a function of grain size. With a decrease in grain size,
205 the soils: a) increase in plagioclase components (e.g., CaO, Al₂O₃) and b) decrease in olivine and
206 pyroxene components (e.g., FeO, MgO). It appears that similar soil-formational processes may
207 occur in the highlands as in the maria. That is, the finest fractions of both the mare and Apollo
208 14 and 16 soils become enriched in plagioclase components. This observation for the mare soils
209 originally led us to conclude [Taylor et al., 2001a, b] that the data appeared to support the Fusion
210 –of-the-Finest Fraction model of agglutinate formation by Papike et al. [1982].

211 There is a systematic and predictable increase of I_S/FeO with decreasing grain size, a result
212 of the increased presence of single-domain, np-Fe⁰, as originally observed by Morris [1978]. Al-
213 though the absolute amount of FeO decreases in the finer fractions, the percentage of this iron
214 that is present in the metallic Fe⁰ state as np-Fe⁰ increases significantly. This is indicated by the
215 large increase in I_S/FeO values with decreasing grain size (Fig. 2), not proportionate to the much
216 smaller increases in the abundances of agglutinitic glass, similar to in the mare soils [Taylor et
217 al., 2001b].

218 **5. Mineral and Glass Chemistry**

219 As part of our extensive characterization of the fine-grain sizes of highland soils, we have
220 determined the average compositions of each of the several phases in the three size fractions. In
221 Table 5, we have presented these compositions for the 20-45 and 10-20 μm fractions of the soils.
222 The precisions associated with these averages are quite large, and we have included the 2σ preci-
223 sions for the agglutinitic glasses, which are by far the largest of all. This illustrates the general
224 findings of several studies of agglutinitic glass in that the compositions actually range between
225 pure plagioclase and that of the mafic minerals, olivine and pyroxene (e.g., Hu and Taylor, 1977).
226 As shown in Figure 3, comparison of the average composition of the agglutinitic glass in the dif-
227 ferent size fractions of a given soil are approximately constant, particularly when the precisions
228 are taken into consideration.

229 With the mare soils (Taylor et al., 2001b), the compositions of the 20-45, 10-20, and <10 μm

230 fractions became progressively similar to the agglutinitic glass, with the glass being higher in
231 plagioclase components (i.e., CaO, Al₂O₃). However, the agglutinitic glass for the highland soils
232 does not demonstrate such a well-defined trend. In fact, the progression from coarse to fine frac-
233 tions has the composition of the size fractions becoming more plagioclase rich, but the agglutinitic
234 glass becomes enriched slightly but distinctly in the mafic components (e.g., FeO, MgO), as
235 illustrated in Figure 3. Although the standard deviation of the average agglutinitic glass compo-
236 sitions is large, the data for highland soils are systematic. These unexpected results, in contrast
237 to those for the mare soils, would appear to indicate that either the F³ model does not adequately
238 explain the formation of the highland soils or some other process, such as an addition of a mare
239 component, has been operative.

240 **5.1 Chemistry of Highland Agglutinates**

241 A perplexing aspect of the chemical data for the highland soils is present when comparing
242 TiO₂ contents of the size separates compared to that of the agglutinitic glass, similar to that for
243 Ti-rich soils [Taylor et al., 2001a, b). Although ilmenite is present in the finest fractions of mare
244 soils in proportions correlated to the type of basalt, the agglutinitic glass was observed to be dep-
245 leted in TiO₂ by more than a factor of two; strongly suggesting ilmenite did not enter the glass in
246 proportion to its abundance in basaltic soils [Pieters et al., 2002].

247 However, the opposite occurs with highland soils. As shown dramatically in Figure 4, the
248 TiO₂ contents of the Apollo 16 agglutinates are distinctly enriched compared to the chemistry of
249 the size-fractions of the soils. In fact, it is not only the TiO₂ contents. The chemistry of the high-
250 land agglutinates in Figure 4, as taken from Table 5, shows that for the Apollo 16 soils, the ag-
251 glutinitic glass has a distinct enrichment in TiO₂, Cr₂O₃, MgO, FeO, and K₂O, compared to the
252 bulk chemistry of each size fraction. This strongly supports the paradigm that there has been
253 large-scale mixing between mare and highlands [Pieters and Taylor, 2003a]. But, it was the glass
254 component of the maria that appears to have been selectively added to the Apollo 16 site. This
255 may well have masked the possible Fusion-of-the-Finest Fraction effects.

256 **6. Visible to Near-infrared Spectroscopy of Highland Soils**

257 Bidirectional reflectance spectra for the bulk soil and size separates are shown for all Apollo
258 14 and 16 soils in Figure 5. The presence of np-Fe⁰ both in the agglutinitic glass and on the sur-
259 faces of grains greatly affects the optical properties of materials exposed to the space environ-

260 ment (e.g., Hapke, 2001; Noble et al., 2001, 2007). The least weathered soils (14141 and 61221)
261 exhibit the most prominent absorption bands diagnostic of the mafic minerals present, largely
262 low-calcium pyroxene. The finest fraction not only contains the lowest abundance of mafic min-
263 erals (Table 2), but it also contains the highest proportion of np-Fe⁰ (Fig 2). Diagnostic absorp-
264 tions are weak or nonexistent in the finest fraction. Similarly, coarse-grained separates contain
265 fewer agglutinates, proportionately greater mafic minerals, and have smaller surface to volume
266 ratios than the finer grained separates. Coarse-grained separates thus always exhibit more promi-
267 nent absorption bands than fine-grained separates from the same soil sample.

268 There is considerable variation of the composition of different size fractions for the same soil
269 (e.g., Fig 2), and it is difficult to reliably quantify the bulk mineralogy for a given soil. Most ab-
270 undance analyses are performed on limited amounts of size fraction, and these data must be used
271 with caution as representations of a soil as a whole. Nevertheless, based on the close similarity
272 of spectra for the 10-20 μm size fraction with the bulk soil seen across Figure 5, this size fraction
273 appears to capture a good balance of diverse competing soil processes. We thus recommend the
274 10-20 μm size fraction be used as a proxy for the bulk when measurements are impractical or
275 impossible for the bulk soil.

276 277 **7. Discussion**

278 The chemistries of the bulk-soil size fractions of the highland soils have similar trends as
279 compared to those of the mare soils. With decreasing grain size, the soil compositions become
280 enriched in plagioclase (CaO, Al₂O₃) and depleted in mafic components (FeO, MgO). The same
281 general trends also exist for both the mare and highland soils with respect to the modal mineral
282 and glass abundances. As with the mare soils, the large increases in the I_S/FeO values, with de-
283 crease in grain size, are not proportional to the more minor increases in abundances of the agglu-
284 tinitic glasses. This large increase in I_S/FeO is attributed to np-Fe⁰ that accumulates on the sur-
285 faces of the soil particles, as discussed for mare soils [Hapke, 2001; Noble et al., 2001; Pieters et
286 al., 2000, 2001; Taylor et al., 2001a, b; Keller and McKay, 1997; Keller et al., 2000; Wentworth
287 et al, 1999].

288 In addition, the unexpected enrichment of the highland agglutinitic glass in mafic components,
289 compared to the compositions of the bulk-soil fractions for Apollo 16 highland soils, has necessi-

290 tated reconsideration of operative processes for the evolution of lunar soils, previously addressed
291 by Pieters and Taylor [2003a]. In particular, the role of selective comminution, lateral mixing,
292 and preferential melting of local components are all clearly important. The suspected large scale
293 mixing between mare and highlands may be real; however, it is the glass chemistry of the mare
294 that is preferentially added to the highlands (i.e., TiO_2 , Cr_2O_3 , MgO , FeO , and K_2O). The rego-
295 lith differential melting sequence, for both highland and mare soils, would appear to be: glass >
296 plagioclase > pyroxene >> ilmenite. Furthermore, it would seem that lunar mafic-rich glass is
297 more likely to melt than Al-rich glass, since mare soils tend to accumulate a higher overall abun-
298 dance of agglutinitic glass than highland soils [Taylor et al., 2001a, b, 2003]. Couple this with
299 the fact that the finer portions of the soil, the ones with dominant agglutinitic glass, are ballisti-
300 cally transported greater distances by impact processes, perhaps enhanced by electrostatic levita-
301 tion [Farrell et al, 2008]. With these considerations in mind, one can readily explain the mare
302 additive to form the FeO-MgO enriched agglutinitic glass of the Apollo 16 highlands.

303 Although we suggest that the source of the mafic glass component in highland soils is the
304 maria in origin, an alternate source for the Apollo 16 soils might be the abundant “mafic impact
305 melt breccias” thought to be derived from Imbrium [Korotev, 1997]. But, here we find it diffi-
306 cult to address the scenario that these melt breccias were selectively and preferentially incorpo-
307 rated into the Apollo 16 agglutinitic glass. Indeed, the Apollo 14 soil chemistry appears to reflect
308 this possible Imbrium component, as seen from their higher K-phase (Fig. 1). However, the
309 model we prefer is necessarily dependent on the small number of sites for which samples are
310 available. It is obvious that we need samples from a highland site far-removed from any maria.

311 **8. Summary**

- 312 ◆ There is a general increase in agglutinitic glass content with decreasing grain size for the
313 highland soils, exactly the same as with the mare soils.
- 314 ◆ The increase in I_S/FeO with decreasing grain size is greater than the abundance of agglutinitic
315 glass: evidence of np-Fe^0 on particle surfaces from vapor deposition (e.g., Hapke et al.,
316 1975).
- 317 ◆ Agglutinitic glass is increased in plagioclase chemical components with decreasing grain
318 size, typical of mare soils, however, not obvious for highland soils.

319 ◆ Apollo 16 agglutinitic glass chemistry contains more “mare-soil components” than the bulk-
320 soil chemistry.

321 ◆ Mare agglutinitic glass appears to have been selectively added to the Apollo 16 soils, perhaps
322 as impact ejecta and/or electrostatically transported fine-grained glass.

323

324

325 **Acknowledgements.** We would like to thank CAPTEM for the allocation of the pristine suite of
326 highland soils. The Curatorial Staff at Johnson Space Center are also thanked for their efficient
327 handling of the distribution of the numerous size fractions of the lunar soils, including the pro-
328 duction of the polished grain mounts. We have benefited from fruitful discussions over the years
329 with Paul Lucey, A. Basu, Sarah Noble, Jim Papike, Amy Riches, and Yang Liu. In addition, it
330 has been the thorough reviews by Drs. Basu and Noble that have been extremely helpful in sub-
331 stantially improving this paper. RELAB at Brown University is a multi-user facility supported
332 under NAG 5-3871. The research presented in this paper was supported by NASA grants from
333 the Cosmochemistry Program to each of the members of the Lunar Soil Characterization Consor-
334 tium (LSCC), for which we are collectively appreciative.

335

336 **References**

- 337 Basu, A., and E. Molinaroli (2001) Sediments of the Moon and Earth as end-members for com-
338 parative planetology. *Earth, Moon, & Planets* 85-86 25-43,
- 339 Basu, A., D.S. McKay, R.V. Morris, and S.J. Wentworth, (1996), Anatomy of individual aggluti-
340 nates from a lunar highland soil, *Meteor. Planet. Sci.*, 31, 777-782.
- 341 Farrell, W. M., T. J. Stubbs, G. T. Delory, R. R. Vondrak, M. R. Collier, J. S. Halekas, and R. P.
342 Lin (2008), Concerning the dissipation of electrically charged objects in the shadowed lunar
343 polar regions, *Geophys. Res. Lett.*, 35, L19104, doi:10.1029/2008GL034785.
- 344 Hapke, B. (2001), Space weathering from Mercury to the asteroid belt. *Jour. Geophys. Res. –*
345 *Planets* 106, 10,039-10,073.
- 346 Hapke, B., W.A. Cassidy, and E.N. Wells (1975), Effects of vapor-phase deposition processes on
347 the optical, chemical, and magnetic properties of the lunar regolith, *Moon*, 13, 339-353
- 348 Hu, H.N., and L.A. Taylor (1977), Lack of chemical fractionation in major and minor elements
349 during agglutinate formation, *Proc. Lunar Planet. Sci. Conf. 8th*, 3645-3656.
- 350 Keller, L.P., and D.S. McKay (1997), The nature and origin of rims on lunar soil grains, *Geo-*
351 *chim. Cosmochim. Acta*, 61, 2331-2340.
- 352 Keller, L.P., S.J. Wentworth, D.S. McKay, L.A. Taylor, C.M. Pieters, and R.V. Morris R.V.
353 (2000), Space weathering in the fine size fraction of lunar soils: Mare/highland differences,
354 *Lunar Planet. Sci. Conf. [CD-Rom]*, XXXI, abstract 1655.
- 355 Korotev, R.L. (1997) Some things we can infer about the Moon from the composition of the
356 Apollo 16 regolith. *Meteor. Planet. Sci.* 32, 447-478.
- 357 McGee, J.J. (1993), Lunar ferroan anorthosites' mineralogy, compositional variations, and petro-
358 genesis. *Jour. Geophys. Res.* 98, 9089-9105,
- 359 Morris, R.V. (1976), Surface exposure indices of lunar soils: A comparative FMR study, *Proc.*
360 *Lunar Planet Sci. Conf. 7th*, 315-335.
- 361 Morris, R.V. (1978), The surface exposure (mature) of lunar soils: Some concepts and Is/FeO
362 compilation, *Proc. Lunar Planet. Sci. Conf. 9th*, 2287-2297.

363 Noble, S.K., C.M. Pieters, L.A. Taylor, R.V. Morris, C.C. Allen, D.S. McKay, and L.P. Keller
364 (2001), The optical properties of the finest fraction of lunar soil: Implications for space wea-
365 thering, *Meteor. Planet. Sci.*, 36, 31-42.

366 Noble, S.K., C.M. Pieters, and L.P. Keller (2007) An experimental approach to understanding the
367 optical effects of space weathering. *Icarus* 192, 629-642.

368 Papike, J.J., S.B. Simon, C. White, and J.C. Laul (1982), The relationship of the lunar regolith
369 <10 μm fraction and agglutinates, Part I, A model for agglutinate formation and some indi-
370 rect supportive evidence, *Proc. Lunar Planet. Sci.* 12, 409-420.

371 Pieters, C.M. (1983), Strength of mineral absorption features in the transmitted component of
372 near-infrared reflected light: First results from RELAB, *J. Geophys. Res.*, 88, 9534-9544.

373 Pieters, C.M. (1993), Compositional diversity and stratigraphy of the lunar crust derived from
374 reflectance spectroscopy, in *Remote Geochemical Analysis: Elemental and Mineralogical*
375 *Composition.*, edited by [C. M. Pieters, and P.A.J. Englert], 309-339, Cambridge Univ.
376 Press, New York.

377 Pieters, C.M. and L.A. Taylor (2002), The perplexing role of TiO_2 in the evolution of lunar soil.
378 *Lunar & Planetary Sci. Conf. XXXIII*, LPI CD-ROM #1886.

379 Pieters, C.M., and L.A. Taylor (2003a), Systematic mixing and melting in lunar soil evolution.
380 *Jour. Geophys. Lett.* 30, 20, 2048, doi:10.1029/2003GL018212.

381 Pieters, C.M., and L.A. Taylor (2003b), The Role of Agglutinates in Lunar Highland Soil Forma-
382 tion , *Lunar & Planet. Sci. XXXIV*, LPI CD-ROM #1223.

383 Pieters, C.M., E.M. Fischer, O. Rode, and A. Basu (1993), Optical effects of space weathering:
384 The role of the finest fraction, *J. Geophys. Res.* 98, 20,817-20,824.

385 Pieters, C.M., L.A. Taylor, S.K. Noble, L.P. Keller, B. Hapke, R.V. Morris, C.C. Allen, and S.
386 Wentworth (2000), Space weathering on airless bodies: Resolving a mystery with lunar
387 samples, *Meteor. Planet. Sci.*, 35, 1101-1107.

388 Pieters C.M., D.G. Stankevich, Y.G. Shkuratov, and L.A. Taylor (2001), Statistical analysis of
389 lunar mare soil mineralogy, chemistry, and reflectance spectra, *Lunar Planet. Sci. Conf.*,
390 [CD-Rom], XXXII, abstract 1783.

391 Pieters, C.M., D.G. Stankevich, Y.G. Shkuratov, and L.A. Taylor (2002), Statistical analysis of
392 the links among lunar mare soil mineralogy, chemistry, and reflectance spectra, *Icarus* 155,
393 285-298.

394 Taylor, L.A., and D.S. McKay (1992), Beneficiation of lunar rocks and regolith: Concepts and
395 difficulties. In Engineering, Construction, Operations in Space III, Vol. I, Eds. Sadeh, Sture
396 and Miller, ASCE, New York, 1058-1069.

397

398 Taylor, L.A., A. Patchen, D.-H. Taylor, J.G. Chambers, and D.S. McKay (1996), X-ray digital
399 imaging and petrography of lunar mare soils: Data input for remote sensing calibrations, *Ica-*
400 *rus*, 124, 500-512.

401 Taylor, L.A. C.M. Pieters, R.V. Morris, L.P. Keller, D.S. McKay, A. Patchen, and S.J. Went-
402 worth (1999), Integration of the chemical and mineralogical characteristics of lunar soils
403 with reflectance spectroscopy, *Proc., Lunar Planet. Sci. Conf.*, [CD-Rom], abstract, 1859.

404 Taylor, L.A., C.M. Pieters, L.P. Keller, R.V. Morris, D.S. McKay, A. Patchen, and S.J. Went-
405 worth (2001a), The effects of space weathering on Apollo 17 mare soils: Petrographic and
406 chemical characterization, *Meteor. Planet. Sci.*, 288-299.

407 Taylor, L.A., Pieters, C.M., Keller, L.P., Morris, R.V., and McKay, D.S. (2001b), Lunar mare
408 soils: Space weathering and the major effects of surface-correlated nanophase Fe. *Jour.*
409 *Geophys. Lett.* 106, 27,985-27,999.

410 Taylor, L.A., Cahill, J.T., Patchen, A., Pieters, C., Morris, R.V., Keller, L.P., & McKay, D.S.
411 (2001c), Mineralogical and chemical characterization of lunar highland regolith: lessons
412 learned from mare soils. *Lunar & Planetary Sci. Conf. XXXII*, LPI CD-OM # 2196.

413 Taylor, L.A., A. Patchen, J. Cahill1, C.M. Pieters, R.V. Morris, L.P. Keller, and D.S. Mckay
414 (2002), Mineral and glass characterization of Apollo 14 soils. *Lunar & Planetary Sci. Conf.*
415 XXXIII, LPI CD-ROM #1302.

416 Taylor, L.A., C.M. Pieters, A. Patchen, D.-H. Taylor, R.V. Morris, L.P. Keller, and D.S. McKay
417 (2003), Mineralogical Characterization of Lunar Highland Soils, *Lunar & Planet. Sci.*
418 XXXIV, LPI CD-ROM #1774.

419 Wentworth, S.J., L.P. Keller, D.S. McKay, and R.V. Morris (1999), Space weathering on the
420 Moon: Patina on Apollo 17 samples 75075 and 76015, *Meteor. Planet. Sci.*, 34, 593-603.

421

TABLES

422
423
424

425
426
427
428

429
430
431
432

433
434
435
436
437
438

439
440
441
442
443

Table 1. Lunar highland soils studies by the Lunar Soil Characterization Consortium (LSCC).

Table 2. Modal abundance of minerals and glasses in finest size fractions of selected Apollo Highland Soils. Maturity as I_s/FeO of the $<250 \mu m$ fraction [Morris, 1978] is given directly after the soil number, a value commonly used as the reference maturity for an entire soil.

Table 3. Modal percentages of four sub-sets of pyroxenes in the finest size fractions of Apollo Highland soils. Maturity as I_s/FeO of the $<250 \mu m$ fraction [Morris, 1978] is given directly after the soil number, a value commonly used as the reference maturity for an entire soil.

Table 4. Bulk chemistry and I_s/FeO values of the finest size fractions of Apollo Highland Soils. The chemistry was determined by EMP analyses of fused beads of the soil. Values of I_s/FeO are from FMR analyses. Maturity as I_s/FeO of the $<250 \mu m$ fraction [Morris, 1978] is given directly after the soil number, a value commonly used as the reference maturity for an entire soil.

Table 5. Average compositions of minerals and glasses in the finest size fractions of Apollo Highland soils. Maturity as I_s/FeO of the $<250 \mu m$ fraction [Morris, 1978] is given directly after the soil number, a value commonly used as the reference maturity for an entire soil. Values in brackets are the 2 sigma error.

444
445

FIGURES

446
447

448
449

450
451
452

453
454
455

Figure 1. Modal analyses of phases in the fine fractions of highland soils. These data are modified after those in a LPSC abstract [Taylor et al., 2003].

Figure 2. Comparisons of oxide components of the bulk chemistry of the fine fractions of highland soils, in addition to their I_s/FeO values

Figure 3. Comparison of chemistry of the agglutinitic glass with the bulk chemistry of the three soil size fractions for Apollo 16 highland soils. Modified from LPSC abstract [Taylor et al., 2003].

Figure 4. Chemistry of soil components relative to the chemistry of the bulk soil ($<45 \mu m$) for representative highland soils. The first three bars (blue shades) are the composition of three soil size separates (see legend). These are followed by the average composition

456 of agglutinitic glass (red shades) present in the indicated size separate. The number in
457 brackets is the I_s/FeO value for the bulk soil from Morris [1978]. Some of these data
458 have been reported in Pieters and Taylor [2003a].

459 Figure 5. Bi-directional reflectance spectra of LSCC highland soils. Data for 64801 are from
460 Pieters and Taylor [2003a].

461

462 TABLE 1. Lunar Highland Soils Studied by the Lunar Soil Characterization Consortium
 463 (LSCC).

464

SAMPLES	Is / FeO*	MATURITY**
Apollo 16	61221	9
	67461	25
	67481	31
	61141	56
	64801	71
	62231	91
Apollo 14	14141	6
	14163	57
	14260	72
	14259	85

465

466 * Values from compilation of Morris [1978] for the <250 μm portion of each soil;

467 ** Maturity based on I_s/FeO [10]; I = Immature = <30 ;

468 S = Submature = 30-60 ; M = Mature = >60.

469

470

471

472 Table 2. Modal abundance of minerals and glasses in finest size fractions of selected Apollo Highland Soils. Maturity as I_S/FeO of the
 473 <250 μm fraction [Morris, 1978] is given directly after the soil number, a value commonly used as the reference maturity for an entire
 474 soil.
 475

	14141^{-5.7}			14163⁻⁵⁷			14260⁻⁷²			14259⁻⁸⁵		
	20-45μm	10-20μm	<10μm	20-45μm	10-20μm	<10μm	20-45μm	10-20μm	<10μm	20-45μm	10-20μm	<10μm
Agglut. Glass	41.0	48.6	45.9	56.4	58.5	66.3	64.0	65.2	66.5	60.5	68.7	71.6
Pyroxene	19.8	10.9	10.3	16.2	13.8	3.8	13.7	12.1	7.7	18.2	9.1	5.9
Plag	26.6	28.0	27.6	18.9	18.3	21.8	15.6	16.1	16.3	14.1	15.4	14.6
Olivine	4.0	1.6	1.5	2.4	2.1	0.4	2.1	1.5	1.4	2.3	1.4	0.7
Ilmenite	1.9	1.1	1.7	0.8	0.9	1.1	0.9	1.0	1.3	1.3	1.2	1.5
K-Phases	4.5	7.4	10.8	3.8	4.1	3.4	2.5	2.6	3.7	2.5	2.7	3.4
Others	2.2	2.4	2.2	1.5	2.3	3.2	1.2	1.5	3.1	1.1	1.5	2.3
Total	100.0	100.0	100.0	100.0	100.0	100.0	100.0	100.0	100.0	100.0	100.0	100.0

476
477

	61221^{-9.2}			67461⁻²⁵			67481⁻³¹			61141⁻⁵⁶		
	20-45μm	10-20μm	<10μm	20-45μm	10-20μm	<10μm	20-45μm	10-20μm	<10μm	20-45μm	10-20μm	<10μm
Agglut. Glass	28.9	32.6	41.6	25.4	32.4	35.8	27.6	28.6	35.2	50.1	53.9	61.6
Pyroxene	7.4	5.3	1.5	7.3	4.1	2.8	6.6	5.6	3.6	4.4	3.3	1.7
Plag	58.7	59.4	54.4	64.3	61.0	60.0	61.2	62.0	58.8	42.5	40.3	35.3
Olivine	3.9	2.0	0.9	2.5	1.5	0.7	4.0	2.9	1.5	2.1	1.6	0.5
Ilmenite	0.6	0.3	0.9	0.3	0.3	0.2	0.1	0.2	0.2	0.3	0.3	0.3
K-Phases	0.2	0.2	0.3	0.1	0.2	0.1	0.3	0.4	0.3	0.3	0.4	0.3
Others	0.3	0.2	0.4	0.1	0.5	0.4	0.2	0.3	0.4	0.3	0.2	0.3
Total	100.0	100.0	100.0	100.0	100.0	100.0	100.0	100.0	100.0	100.0	100.0	100.0

478

	64801⁻⁸²			62231⁻⁹¹		
	20-45μm	10-20μm	<10μm	20-45μm	10-20μm	<10μm
Agglut. Glass	53.6	61.0	63.6	50.6	55.0	69.5
Pyroxene	4.5	2.8	2.7	5.1	4.40	0.9
Plag	39.3	34.5	32.3	40.5	37.8	28.3
Olivine	1.8	1.0	0.6	2.9	1.7	0.3
Ilmenite	0.3	0.2	0.2	0.3	0.5	0.4
K-Phases	0.3	0.3	0.4	0.3	0.4	0.3
Others	0.2	0.2	0.2	0.3	0.2	0.3
Total	100.0	100.0	100.0	100.0	100.0	100.0

479

480 Table 3. Modal percentages of four sub-sets of pyroxenes in the finest size fractions of Apollo Highland soils. Maturity as I_s/FeO of the
 481 <250 μm fraction [Morris, 1978] is given directly after the soil number, a value commonly used as the reference maturity for an entire
 482 soil.

483

	14141-5.7			14163-57			14260-72			14259-85		
	20-45μm	10-20μm	<10μm	20-45μm	10-20μm	<10μm	20-45μm	10-0μm	<10μm	20-45μm	10-20μm	<10μm
Orthopyroxene	7.57	4.07	3.37	6.50	5.68	1.51	4.68	5.14	2.58	7.40	3.72	1.92
Pigeonite	8.08	4.58	4.29	5.66	4.94	1.38	4.99	4.23	3.15	6.14	3.18	1.96
Mg-Clinopyroxene	3.08	1.85	2.19	3.10	2.41	0.91	3.07	2.00	1.51	3.04	1.66	1.77
Fe-Pyroxene	1.08	0.38	0.44	0.92	0.78	0.14	0.94	0.64	0.48	1.57	0.50	0.29
Total Pyroxene	19.81	10.88	10.29	16.18	13.81	3.94	13.68	12.01	7.72	18.15	9.06	5.94

484

	61221-9.2			67461-25			67481-31			61141-56		
	20-45μm	10-20μm	<10μm	20-45μm	10-20μm	<10μm	20-45μm	10-0μm	<10μm	20-45μm	10-20μm	<10μm
Orthopyroxene	2.96	1.82	0.56	2.96	1.47	1.09	2.95	2.55	1.38	1.68	1.69	0.22
Pigeonite	2.24	1.43	0.55	1.61	1.07	0.64	1.54	1.27	1.05	1.38	2.15	0.23
Mg-Clinopyroxene	1.98	1.95	0.37	2.53	1.52	1.06	1.94	1.73	1.41	1.11	1.45	0.19
Fe-Pyroxene	0.19	0.14	0.02	0.18	0.05	0.04	0.17	0.13	0.05	0.18	0.04	0.06
Total Pyroxene	7.37	5.34	1.50	7.28	4.11	2.83	6.60	5.68	3.89	4.35	5.33	0.70

486

	64801-82			62231-91		
	20-45μm	10-20μm	<10μm	20-45μm	10-20μm	<10μm
Orthopyroxene	2.03	1.24	1.18	2.08	1.99	0.28
Pigeonite	1.15	0.96	0.84	1.33	1.55	0.27
Mg-Clinopyroxene	1.33	0.60	0.64	1.52	1.74	0.30
Fe-Pyroxene	0.01	0.01	0.00	0.19	0.12	0.03
Total Pyroxene	4.52	2.81	2.66	5.12	5.40	0.88

487

488

489
490
491
492

Table 4. Bulk chemistry and I_s/FeO values of the finest size fractions of Apollo Highland Soils. The chemistry was determined by EMP analyses of fused beads of the soil. Values of I_s/FeO are from FMR analyses. Maturity as I_s/FeO of the $<250 \mu m$ fraction [Morris, 1978] is given directly after the soil number, a value commonly used as the reference maturity for an entire soil.

Sample	14141-5.7				14163-57				14260-72			
	<45 μm	20-45 μm	10-20 μm	<10 μm	<45 μm	20-45 μm	10-20 μm	<10 μm	<45 μm	20-45 μm	10-20 μm	<10 μm
SiO ₂	47.9	47.2	48.4	49.2	47.4	47.1	47.4	47.2	47.6	47.4	47.5	47.8
TiO ₂	1.65	1.96	1.71	1.51	1.90	2.00	1.88	2.07	1.85	1.86	1.98	1.94
Al ₂ O ₃	17.0	15.0	17.2	19.2	17.1	15.4	17.0	18.9	17.3	16.3	17.3	19.1
Cr ₂ O ₃	0.22	0.26	0.23	0.21	0.20	0.23	0.22	0.21	0.21	0.22	0.23	0.20
MgO	9.28	11.0	9.08	6.99	9.49	11.0	9.57	8.14	9.46	10.4	9.53	8.21
CaO	10.7	10.1	10.7	11.3	10.9	10.2	10.8	11.6	11.0	10.7	11.0	11.8
MnO	0.14	0.15	0.13	0.10	0.15	0.15	0.13	0.12	0.15	0.14	0.13	0.12
FeO	9.81	11.6	9.46	7.66	9.94	11.5	10.1	8.83	9.65	10.7	9.84	8.10
Na ₂ O	0.76	0.59	0.71	0.91	0.65	0.57	0.67	0.70	0.61	0.60	0.60	0.57
K ₂ O	0.70	0.47	0.66	0.96	0.51	0.41	0.51	0.55	0.49	0.44	0.46	0.47
P ₂ O ₅	0.50	0.26	0.32	0.40	0.35	0.21	0.27	0.33	0.32	0.22	0.21	0.17
SO ₃	0.10	0.07	0.07	0.10	0.10	0.08	0.10	0.11	0.12	0.10	0.10	0.09
Total	98.82	98.78	98.68	98.61	98.69	99.02	98.72	98.85	98.81	99.13	98.97	98.76
I_s/FeO	9.7	5.8	11.6	14.5	66.5	43.2	64.8	87.0	93.3	80.2	98.9	144.9

493
494

Sample	14259-85				61221-9.2				67461-25			
	<45 μm	20-45 μm	10-20 μm	<10 μm	<45 μm	20-45 μm	10-20 μm	<10 μm	<45 μm	20-45 μm	10-20 μm	<10 μm
SiO ₂	47.7	47.1	47.5	47.9	44.7	44.5	44.5	44.5	44.6	44.4	44.1	44.5
TiO ₂	1.80	1.99	1.96	2.02	0.52	0.56	0.54	0.50	0.35	0.44	0.39	0.34
Al ₂ O ₃	17.4	15.8	17.4	19.3	27.3	27.2	27.5	28.5	28.4	27.3	27.8	29.4
Cr ₂ O ₃	0.20	0.24	0.23	0.20	0.09	0.09	0.09	0.08	0.08	0.09	0.08	0.08
MgO	9.47	10.7	9.44	8.09	5.29	5.45	5.16	4.35	4.46	5.11	4.80	3.83
CaO	11.1	10.5	11.0	11.9	15.9	15.9	16.0	16.5	16.5	16.1	16.5	17.1
MnO	0.13	0.15	0.13	0.12	0.08	0.06	0.05	0.06	0.06	0.07	0.08	0.06
FeO	9.54	11.0	9.71	7.82	4.47	4.62	4.40	3.64	4.24	4.93	4.64	3.35
Na ₂ O	0.62	0.60	0.63	0.63	0.48	0.46	0.45	0.53	0.40	0.41	0.39	0.43
K ₂ O	0.47	0.43	0.47	0.50	0.09	0.07	0.09	0.13	0.06	0.05	0.05	0.07
P ₂ O ₅	0.30	0.26	0.23	0.23	0.06	0.05	0.05	0.06	0.04	0.03	0.04	0.03
SO ₃	0.11	0.09	0.12	0.10	0.07	0.04	0.06	0.10	0.06	0.07	0.04	0.07
Total	98.80	99.02	98.87	98.84	99.13	99.07	98.93	99.00	99.26	99.00	98.90	99.31
I_s/FeO	108.6	77.2	101.8	174.8	13.6	8.4	13.89	19.8	29.8	22.3	23.9	35.2

495
496
497
498
499

500

501
502
503

Table 4 continued

Sample	67481-31				61141-56				64801-82			
	<45µm	20-45µm	10-20µm	<10µm	<45µm	20-45µm	10-20µm	<10µm	<45µm	20-45µm	10-20µm	<10µm
SiO ₂	44.6	44.7	44.4	44.5	45.0	44.5	44.6	44.9	45.0	44.6	44.5	44.8
TiO ₂	0.44	0.49	0.40	0.42	0.59	0.58	0.64	0.59	0.65	0.63	0.68	0.61
Al ₂ O ₃	28.1	26.7	28.4	29.1	26.3	26.1	25.6	27.4	26.9	26.5	26.3	27.7
Cr ₂ O ₃	0.10	0.09	0.09	0.08	0.12	0.11	0.13	0.11	0.10	0.10	0.12	0.12
MgO	4.91	5.98	4.54	4.09	6.39	6.56	6.84	5.53	5.83	6.09	6.18	5.22
CaO	16.2	15.6	16.4	16.7	15.3	15.2	15.2	16.0	15.6	15.6	15.6	16.1
MnO	0.06	0.08	0.05	0.07	0.07	0.08	0.08	0.07	0.06	0.08	0.08	0.07
FeO	4.38	5.19	4.04	3.61	4.80	5.15	5.14	3.66	4.68	4.82	4.78	3.84
Na ₂ O	0.43	0.45	0.45	0.46	0.43	0.46	0.41	0.48	0.43	0.44	0.41	0.42
K ₂ O	0.06	0.06	0.07	0.08	0.11	0.10	0.10	0.14	0.12	0.12	0.11	0.14
P ₂ O ₅	0.04	0.05	0.04	0.04	0.06	0.06	0.05	0.06	0.07	0.06	0.06	0.04
SO ₃	0.04	0.04	0.06	0.07	0.09	0.05	0.08	0.11	0.09	0.10	0.07	0.11
Total	99.39	99.50	99.08	99.22	99.34	99.00	98.91	99.11	99.50	99.20	98.99	99.21
I_s/FeO	33.5	20.7	33.0	38.5	94.5	75.5	81.6	119.3	92.2	83.4	84.9	115.2

504

Sample	62231-91			
	<45µm	20-45µm	10-20µm	<10µm
SiO ₂	45.0	44.5	44.7	45.0
TiO ₂	0.60	0.58	0.61	0.58
Al ₂ O ₃	26.3	25.7	26.3	27.4
Cr ₂ O ₃	0.11	0.11	0.13	0.13
MgO	6.20	6.59	6.38	5.49
CaO	15.4	15.3	15.5	16.1
MnO	0.09	0.09	0.07	0.07
FeO	4.87	5.31	4.86	3.63
Na ₂ O	0.43	0.42	0.41	0.46
K ₂ O	0.12	0.09	0.10	0.14
P ₂ O ₅	0.07	0.07	0.05	0.04
SO ₃	0.09	0.08	0.08	0.13
Total	99.32	98.87	99.22	99.22
I_s/FeO	116.7	80.7	109.9	169.0

505
506

507 Table 5. Average compositions of minerals and glasses in the finest size fractions of Apollo Highland soils.
 508 Maturity as I_5/FeO of the <250 μm fraction [Morris, 1978] is given directly after the soil number, a value commonly used as the reference
 509 maturity for an entire soil. Values in brackets are the 2 sigma error.

510

14141 -5.7 (20-45μm)									
	Plag	Ilm	Olivine	K-glass	Agglut. Gls.	Opx	Pig	Mg-Cpx	Fe-Cpx
SiO₂	45.7	<0.04	36.2	70.1	47.0 (37)	52.8	51.6	49.9	46.9
TiO₂	<0.04	52.4	0.07	0.27	1.82 (208)	0.68	0.74	1.30	1.06
Al₂O₃	33.5	0.10	0.06	13.7	17.9 (75)	1.03	1.51	1.74	1.32
Cr₂O₃	<0.04	0.61	0.08	<0.04	0.18 (11)	0.36	0.47	0.46	0.21
MgO	0.09	3.42	31.8	0.31	7.98 (441)	24.6	20.5	13.8	6.72
CaO	17.6	0.17	0.15	1.16	11.4 (34)	1.84	4.59	15.1	10.3
FeO	0.06	40.8	30.1	1.21	9.76 (608)	17.3	19.0	16.0	30.9
Na₂O	1.22	<0.04	<0.04	0.86	0.74 (51)	<0.04	<0.04	0.07	<0.04
K₂O	0.16	<0.04	<0.04	8.81	0.46 (54)	<0.04	<0.04	<0.04	<0.04
Total	98.33	97.50	98.46	96.42	97.24	98.61	98.41	98.37	97.41

511
512

14141 -5.7 (10-20 μm)									
	Plag	Ilm	Olivine	K-glass	Agglut. Gls.	Opx	Pig	Mg-Cpx	Fe-Cpx
SiO₂	45.2	<0.04	36.6	72.0	46.8 (41)	52.7	51.7	50.0	46.7
TiO₂	0.06	52.3	0.11	0.39	1.69 (180)	0.76	0.78	1.51	1.23
Al₂O₃	34.0	0.14	0.14	12.1	19.3 (64)	1.02	1.37	1.98	1.39
Cr₂O₃	<0.04	0.56	0.08	<0.04	0.20 (12)	0.34	0.45	0.56	0.18
MgO	0.13	3.33	32.8	0.12	7.91 (369)	24.2	20.6	14.6	5.73
CaO	18.0	0.20	0.15	1.96	11.9 (32)	1.99	4.33	16.2	10.6
FeO	0.17	40.6	28.9	3.31	8.81 (417)	17.4	19.2	13.0	31.8
Na₂O	1.07	<0.04	<0.04	1.49	0.74 (59)	<0.04	<0.04	0.10	<0.04
K₂O	0.15	0.05	<0.04	5.45	0.39 (41)	<0.04	<0.04	<0.04	<0.04
Total	98.78	97.18	98.78	96.82	97.80	98.41	98.43	97.95	97.63

513
514

515
516
517

Table 5. Continued

14163 -57 (20-45µm)									
	Plag	Ilm	Olivine	K-glass	Agglut. Gls.	Opx	Pig	Mg-Cpx	Fe-Cpx
SiO₂	46.2	<0.04	36.7	67.6	46.8 (30)	52.9	51.5	50.6	46.8
TiO₂	0.04	51.6	0.08	0.43	1.71 (138)	0.75	0.67	1.27	0.94
Al₂O₃	32.9	0.16	0.04	14.8	17.2 (61)	1.30	1.46	1.70	1.01
Cr₂O₃	<0.04	0.65	0.05	<0.04	0.17 (13)	0.32	0.39	0.39	0.12
MgO	0.04	2.17	34.3	0.54	8.64 (394)	24.2	18.1	13.9	4.97
CaO	17.6	0.25	0.16	2.25	11.4 (28)	2.00	5.17	16.6	11.0
FeO	0.06	42.3	26.8	1.90	10.2 (49)	16.8	21.0	13.8	32.7
Na₂O	1.38	<0.04	<0.04	1.21	0.58 (39)	<0.04	0.04	0.13	0.05
K₂O	0.18	0.04	<0.04	8.40	0.43 (44)	<0.04	<0.04	<0.04	<0.04
Total	98.4	97.17	98.13	97.13	97.03	98.27	98.33	98.39	97.59

518
519
520

14163 -57 (10-20µm)									
	Plag	Ilm	Olivine	Vol Gls.	Agglut. Gls.	Opx	Pig	Mg-Cpx	Fe-Cpx
SiO₂	45.8	0.12	36.8	67.9	46.4 (28)	52.9	51.4	50.4	47.6
TiO₂	<0.04	52.0	0.08	0.30	1.66 (123)	0.75	0.68	1.38	1.04
Al₂O₃	33.6	0.19	0.09	15.2	18.1 (63)	1.10	1.18	1.90	1.24
Cr₂O₃	<0.04	0.45	0.11	<0.04	0.19 (37)	0.31	0.38	0.48	0.18
MgO	0.08	3.95	33.3	0.14	8.64 (353)	24.8	19.4	14.7	7.52
CaO	17.6	0.26	0.24	1.73	11.6 (28)	1.88	4.68	17.2	10.8
FeO	0.22	39.5	27.9	1.83	9.65 (438)	16.4	20.3	12.1	29.0
Na₂O	1.33	<0.04	<0.04	1.23	0.59 (40)	<0.04	<0.04	0.13	0.06
K₂O	0.14	<0.04	<0.04	8.64	0.36 (39)	<0.04	<0.04	<0.04	<0.04
Total	98.77	96.47	98.52	96.97	97.19	98.14	98.02	98.29	97.44

521
522

523
524
525
526
527

Table 5. Cont.

14260 -72 (20-45µm)									
	Plag	Ilm	Olivine	Vol Gls.	Agglut. Gls.	Opx	Pig	Mg-Cpx	Fe-Cpx
SiO₂	45.6	0.07	36.7	68.6	46.3 (37)	52.8	50.9	50.1	47.1
TiO₂	0.05	52.4	0.09	0.38	1.54 (113)	0.79	0.88	1.50	1.01
Al₂O₃	33.7	0.06	0.05	15.8	18.6 (66)	1.06	1.63	2.10	1.15
Cr₂O₃	<0.04	0.50	0.12	<0.04	0.21 (15)	0.35	0.47	0.58	0.24
MgO	0.09	3.54	32.8	0.10	8.42 (418)	24.5	18.3	14.7	6.91
CaO	17.6	0.19	0.17	2.07	11.6 (31)	1.86	5.28	16.6	12.3
FeO	0.18	40.5	29.1	0.27	9.64 (487)	17.3	21.1	12.6	28.6
Na₂O	1.22	<0.04	<0.04	1.09	0.60 (45)	<0.04	<0.04	0.12	0.0
K₂O	0.14	<0.04	<0.04	8.96	0.41 (45)	<0.04	<0.04	<0.04	<0.04
Total	98.58	97.26	99.03	97.27	97.26	98.66	98.56	98.30	97.31

528
529
530

14260 -72 (10-20µm)									
	Plag	Ilm	Olivine	Vol Gls.	Agglut. Gls.	Opx	Pig	Mg-Cpx	Fe-Cpx
SiO₂	45.8	0.10	36.9	66.3	45.5 (44)	53.0	51.1	50.8	47.8
TiO₂	0.05	51.3	0.10	0.32	1.62 (125)	0.80	0.82	1.30	1.12
Al₂O₃	33.8	0.18	0.08	15.6	19.9 (71)	1.04	1.17	1.89	1.37
Cr₂O₃	<0.04	0.53	0.09	<0.04	0.22 (11)	0.32	0.33	0.50	0.18
MgO	0.08	3.25	32.9	0.61	8.39 (401)	24.1	18.6	15.0	7.01
CaO	17.6	0.24	0.19	2.31	12.4 (34)	1.92	4.94	16.4	12.7
FeO	0.28	40.8	29.2	2.05	8.85 (434)	17.9	21.4	12.9	28.1
Na₂O	1.28	<0.04	<0.04	0.79	0.53 (42)	<0.04	<0.04	0.08	<0.04
K₂O	0.15	0.06	<0.04	8.42	0.40 (48)	<0.04	<0.04	<0.04	<0.04
Total	99.04	97.46	99.46	96.40	97.90	99.08	98.36	98.87	98.28

531
532
533

534
535
536
537
538

Table 5. Cont.

14259 –85 (20-45µm)									
	Plag	Ilm	Olivine	Vol Gls.	Agglut. Gls.	Opx	Pig	Mg-Cpx	Fe-Cpx
SiO₂	46.3	<0.04	36.9	68.7	46.5 (33)	53.0	51.4	50.3	46.9
TiO₂	0.05	52.8	0.10	0.69	1.50 (118)	0.75	0.75	1.42	1.01
Al₂O₃	33.5	0.09	0.06	14.8	19.2 (63)	0.98	1.22	2.00	1.09
Cr₂O₃	<0.04	0.52	0.11	<0.04	0.19 (11)	0.35	0.44	0.53	0.19
MgO	0.10	3.23	33.1	0.21	8.38 (378)	24.5	19.0	14.6	5.03
CaO	17.3	0.11	0.18	1.82	12.0 (29)	1.83	5.10	16.2	11.2
FeO	0.05	41.1	28.8	1.30	9.17 (459)	17.5	20.7	13.3	32.5
Na₂O	1.41	<0.04	<0.04	1.02	0.61 (66)	<0.04	<0.04	0.11	<0.04
K₂O	0.20	<0.04	<0.04	8.57	0.37 (43)	<0.04	<0.04	<0.04	<0.04
Total	98.91	97.85	99.25	97.11	97.80	98.91	98.61	98.46	97.92

539
540

14259 –85 (10-20µm)									
	Plag	Ilm	Olivine	Vol Gls.	Agglut. Gls.	Opx	Pig	Mg-Cpx	Fe-Cpx
SiO₂	45.8	0.08	36.8	72.8	45.8 (31)	52.4	50.9	50.2	46.8
TiO₂	<0.04	52.4	0.05	0.45	1.64 (135)	0.90	0.77	0.92	0.99
Al₂O₃	33.5	0.11	0.05	11.8	18.7 (57)	1.02	1.11	2.68	1.21
Cr₂O₃	<0.04	0.42	<0.04	<0.04	0.16 (11)	0.27	0.32	0.73	0.18
MgO	0.05	3.63	33.3	0.09	8.33 (291)	23.5	18.4	15.4	5.81
CaO	17.4	0.16	0.16	1.24	11.8 (24)	1.93	4.83	14.4	12.2
FeO	0.10	39.6	27.7	2.16	9.81 (445)	17.7	21.1	13.6	29.5
Na₂O	1.34	<0.04	<0.04	0.73	0.55 (40)	<0.04	<0.04	0.07	0.05
K₂O	0.10	<0.04	<0.04	7.49	0.36 (39)	<0.04	<0.04	<0.04	<0.04
Total	98.29	96.40	98.06	96.76	97.09	97.72	97.43	98.00	96.74

541
542

543
544
545
546
547

Table 5. Cont.

61221 -9.2 (20-45µm)									
	Plag	Ilm	Olivine	Vol Gls.	Agglut. Gls.	Opx	Pig	Mg-Cpx	Fe-Cpx
SiO₂	44.2	<0.04	37.7	46.4	45.1 (31)	53.0	51.6	50.8	45.0
TiO₂	<0.04	52.9	0.08	0.91	1.12 (185)	0.61	0.78	1.37	0.78
Al₂O₃	35.3	0.18	0.15	1.10	24.2 (80)	1.06	1.22	1.99	0.95
Cr₂O₃	<0.04	0.47	<0.04	<0.04	0.09 (13)	0.29	0.27	0.52	<0.04
MgO	<0.04	2.88	36.8	0.68	6.57 (485)	24.4	19.6	14.8	0.68
CaO	19.0	0.09	0.11	18.9	14.3 (35)	1.56	4.78	18.1	7.69
FeO	0.07	41.1	24.5	30.1	6.24 (557)	18.0	20.4	11.4	42.4
Na₂O	0.56	<0.04	<0.04	0.14	0.54 (42)	<0.04	0.05	0.09	<0.04
K₂O	<0.04	<0.04	<0.04	<0.04	0.16 (29)	<0.04	<0.04	<0.04	<0.04
Total	99.13	97.62	99.34	98.23	98.30	98.92	98.70	99.07	97.50

548
549

61221 -9.2 (10-20µm)									
	Plag	Ilm	Olivine	Vol Gls.	Agglut. Gls.	Opx	Pig	Mg-Cpx	Fe-Cpx
SiO₂	44.1	0.08	38.0	65.9	45.3 (41)	53.3	51.9	51.0	48.6
TiO₂	<0.04	51.8	0.07	1.16	1.00 (170)	0.60	0.68	1.01	0.89
Al₂O₃	34.9	0.10	0.08	12.1	23.1 (77)	0.95	1.16	1.48	1.11
Cr₂O₃	<0.04	0.44	0.05	0.08	0.13 (15)	0.34	0.36	0.42	0.14
MgO	0.07	2.57	37.0	1.58	7.37 (484)	24.8	20.4	14.6	8.37
CaO	19.1	0.42	0.19	2.69	13.9 (36)	1.65	4.01	18.7	14.3
FeO	0.16	41.9	24.0	4.66	6.98 (545)	17.64	20.4	11.4	24.8
Na₂O	0.58	<0.04	<0.04	1.42	0.43 (34)	<0.04	<0.04	0.07	0.07
K₂O	0.04	0.05	<0.04	6.37	0.14 (26)	<0.04	<0.04	<0.04	<0.04
Total	98.95	97.36	99.39	95.96	98.37	99.28	98.91	98.68	98.28

550
551

552
553
554
555
556

Table 5. Cont.

67461 -25 (20-45µm)									
	Plag	Ilm	Olivine	Vol Gls.	Agglut. Gls.	Opx	Pig	Mg-Cpx	Fe-Cpx
SiO₂	44.0	0.04	36.1	72.7	43.9 (43)	53.3	52.1	50.5	46.4
TiO₂	<0.04	52.4	0.06	0.35	0.53 (55)	0.56	0.51	1.06	0.82
Al₂O₃	35.0	0.07	<0.04	9.74	24.6 (79)	0.99	1.27	1.53	0.72
Cr₂O₃	<0.04	0.20	0.04	<0.04	0.15 (48)	0.38	0.42	0.56	0.05
MgO	0.06	2.33	30.9	0.12	7.47 (547)	25.4	22.3	14.3	4.01
CaO	19.2	0.22	0.11	0.47	14.6 (37)	1.52	4.51	19.0	15.7
FeO	0.15	42.4	31.9	5.26	6.48 (481)	16.9	17.3	11.5	28.0
Na₂O	0.54	<0.04	<0.04	0.11	0.40 (24)	<0.04	<0.04	0.06	0.04
K₂O	<0.04	<0.04	<0.04	7.11	0.08 (17)	<0.04	<0.04	<0.04	-----
Total	98.95	97.66	99.11	95.86	98.26	99.05	98.41	98.51	95.74

557
558
559

67461 -25 (10-20µm)									
	Plag	Ilm	Olivine	Vol Gls.	Agglut. Gls.	Opx	Pig	Mg-Cpx	Fe-Cpx
SiO₂	44.3	0.04	36.6	73.4	43.7 (48)	52.7	51.9	50.8	47.5
TiO₂	<0.04	52.7	0.05	0.35	0.55 (35)	0.51	0.55	1.01	0.83
Al₂O₃	34.6	0.09	<0.04	9.92	24.9 (67)	0.79	1.36	1.43	0.75
Cr₂O₃	<0.04	0.22	0.04	<0.04	0.15 (23)	0.43	0.43	0.53	0.05
MgO	0.07	2.38	31.0	0.10	7.28 (497)	25.6	22.9	14.8	4.21
CaO	19.3	0.23	0.11	0.42	13.9 (47)	1.15	4.54	18.6	15.8
FeO	0.18	42.7	31.7	5.12	6.63 (453)	16.7	17.0	11.4	29.5
Na₂O	0.55	<0.04	<0.04	0.13	0.36 (19)	<0.04	<0.04	0.05	0.04
K₂O	<0.04	<0.04	<0.04	7.81	0.07 (11)	<0.04	<0.04	<0.04	-----
Total	99.00	98.36	99.50	97.25	97.54	97.88	98.68	98.62	98.64

560
561

562
563
564
565
566

Table 5. Cont.

67481 -31 (20-45µm)									
	Plag	Ilm	Olivine	Vol Gls.	Agglut. Gls.	Opx	Pig	Mg-Cpx	Fe-Cpx
SiO₂	44.2	0.09	36.9	68.9	44.3 (36)	52.6	52.8	51.1	47.6
TiO₂	<0.04	53.1	0.08	0.27	0.76 (301)	0.53	0.59	1.14	1.33
Al₂O₃	35.0	<0.04	0.08	15.3	25.6 (69)	0.85	0.85	1.51	0.79
Cr₂O₃	<0.04	0.23	0.06	<0.04	0.14 (15)	0.33	0.32	0.55	0.17
MgO	0.06	2.81	33.1	0.10	6.53 (502)	23.3	22.2	14.3	4.49
CaO	19.1	0.10	0.07	1.31	15.1 (35)	1.40	4.42	18.5	17.1
FeO	0.06	42.6	29.3	0.09	5.59 (490)	19.9	18.0	11.9	27.1
Na₂O	0.56	0.04	<0.04	0.32	0.43 (22)	<0.04	<0.04	0.09	0.11
K₂O	0.06	0.04	<0.04	10.7	0.08 (10)	<0.04	<0.04	<0.04	<0.04
Total	99.04	99.01	99.59	96.99	98.51	98.91	99.18	99.09	98.69

567
568

67481-31 (10-20µm)									
	Plag	Ilm	Olivine	Vol Gls.	Agglut. Gls.	Opx	Pig	Mg-Cpx	Fe-Cpx
SiO₂	44.6	0.07	37.1	70.5	44.5 (38)	53.1	53.1	51.7	48.4
TiO₂	<0.04	52.8	0.07	0.37	0.85 (138)	0.59	0.61	0.94	0.90
Al₂O₃	34.6	<0.04	<0.04	14.3	24.6 (69)	0.79	0.96	1.30	0.70
Cr₂O₃	<0.04	0.31	0.07	<0.04	0.13 (13)	0.34	0.31	0.44	0.05
MgO	0.08	2.58	33.9	<0.04	7.03 (446)	24.3	22.0	14.9	5.04
CaO	18.9	0.25	0.14	1.71	14.7 (32)	1.69	3.96	19.3	16.8
FeO	0.15	42.0	28.2	0.43	6.20 (468)	18.3	18.8	10.8	26.6
Na₂O	0.65	<0.04	<0.04	0.67	0.44 (54)	<0.04	<0.04	0.05	0.06
K₂O	0.06	<0.04	<0.04	9.11	0.18 (73)	<0.04	<0.04	<0.04	<0.04
Total	99.04	98.01	99.48	97.09	98.64	99.11	99.74	99.43	98.55

569
570

571
572
573
574
575

Table 5. Cont.

61141 -56 (20-45µm)									
	Plag	Ilm	Olivine	Vol Gls.	Agglut. Gls.	Opx	Pig	Mg-Cpx	Fe-Cpx
SiO₂	44.3	<0.04	37.7	71.5	44.2 (41)	52.8	52.2	51.4	45.2
TiO₂	<0.04	53.4	0.06	0.35	1.05 (169)	0.66	0.61	0.85	0.89
Al₂O₃	34.9	0.06	0.06	14.4	23.5 (83)	0.86	0.97	1.29	0.87
Cr₂O₃	<0.04	0.38	0.07	<0.04	0.16 (16)	0.33	0.33	0.40	0.08
MgO	0.04	3.78	37.7	0.15	7.52 (516)	24.6	21.3	15.1	0.69
CaO	18.9	0.13	0.11	1.55	14.3 (37)	1.61	4.62	20.0	10.4
FeO	0.10	40.8	23.5	0.68	7.17 (583)	18.0	18.8	9.57	39.8
Na₂O	0.70	<0.04	<0.04	0.86	0.40 (28)	<0.04	<0.04	0.07	<0.04
K₂O	0.05	<0.04	<0.04	7.70	0.11 (25)	<0.04	<0.04	<0.04	<0.04
Total	98.99	98.65	99.20	97.19	98.47	98.86	98.83	98.68	97.93

576
577

61141 -56 (10-20µm)									
	Plag	Ilm	Olivine	Vol Gls.	Agglut. Gls.	Opx	Pig	Mg-Cpx	Fe-Cpx
SiO₂	44.4	0.07	37.8	74.2	44.5 (41)	53.6	52.6	51.0	44.9
TiO₂	0.05	52.9	0.10	0.17	0.88 (129)	0.72	0.80	1.15	0.84
Al₂O₃	34.6	<0.04	<0.04	11.7	23.9 (72)	1.05	1.05	1.39	0.97
Cr₂O₃	<0.04	0.44	0.06	<0.04	0.14 (12)	0.44	0.43	0.38	0.09
MgO	0.07	2.96	37.3	0.42	7.60 (448)	25.8	22.5	14.3	1.03
CaO	19.0	0.21	0.13	0.64	14.5 (33)	1.75	4.51	19.1	10.7
FeO	0.17	41.7	24.2	1.63	6.75 (445)	16.1	17.2	11.5	39.9
Na₂O	0.68	<0.04	<0.04	1.32	0.42 (38)	<0.04	<0.04	0.09	<0.04
K₂O	0.07	<0.04	<0.04	8.40	0.14 (26)	<0.04	<0.04	<0.04	<0.04
Total	99.04	98.28	99.59	98.48	98.75	99.46	99.09	98.91	98.43

578
579

580
581
582
583
584

Table 5. Cont.

64801 -82 (20-45µm)									
	Plag	Ilm	Olivine	Vol Gls.	Agglut. Gls.	Opx	Pig	Mg-Cpx	Fe-Cpx
SiO₂	44.1	0.06	37.7	73.5	45.5 (38)	53.3	51.4	50.8	48.6
TiO₂	<0.04	53.3	0.07	0.39	1.02 (143)	0.78	0.73	1.34	0.36
Al₂O₃	34.7	0.15	0.06	12.1	22.7 (78)	1.17	1.12	1.84	0.59
Cr₂O₃	<0.04	0.39	0.08	<0.04	0.13 (12)	0.41	0.36	0.56	0.24
MgO	<0.04	4.01	37.1	<0.04	6.97 (503)	26.1	19.6	15.3	5.40
CaO	19.3	0.22	0.15	0.93	13.9 (36)	1.84	4.75	18.5	19.3
FeO	0.07	40.4	24.1	1.64	7.02 (502)	15.5	20.6	10.4	23.9
Na₂O	0.47	<0.04	<0.04	0.93	0.42 (35)	<0.04	<0.04	0.09	0.08
K₂O	<0.04	0.04	<0.04	7.93	0.21 (58)	<0.04	<0.04	<0.04	<0.04
Total	98.64	98.57	99.26	97.42	97.97	99.10	98.56	98.83	98.47

585
586

64801 -82 (10-20µm)									
	Plag	Ilm	Olivine	Vol Gls.	Agglut. Gls.	Opx	Pig	Mg-Cpx	Fe-Cpx
SiO₂	43.9	0.04	37.7	70.8	44.8 (31)	53.5	52.4	50.6	48.4
TiO₂	<0.04	52.6	0.08	0.62	0.76 (98)	0.66	0.78	1.74	0.83
Al₂O₃	34.7	0.06	<0.04	12.7	23.8 (71)	1.18	1.15	2.14	1.20
Cr₂O₃	<0.04	0.56	0.08	<0.04	0.13 (13)	0.41	0.38	0.54	0.08
MgO	0.07	2.77	37.4	0.52	7.24 (460)	26.4	22.6	15.9	6.58
CaO	19.3	0.32	0.18	2.02	14.3 (34)	1.74	4.48	17.7	15.9
FeO	0.15	41.7	23.7	3.03	6.41 (446)	15.1	17.0	10.2	25.4
Na₂O	0.51	<0.04	<0.04	0.72	0.42 (47)	<0.04	<0.04	0.09	0.08
K₂O	<0.04	<0.04	<0.04	5.81	0.19 (46)	<0.04	<0.04	<0.04	<0.04
Total	98.63	98.05	99.14	96.22	98.09	98.99	98.79	98.91	98.47

587
588

589
590
591
592
593

Table 5. Cont.

62231 -91 (20-45µm)									
	Plag	Ilm	Olivine	Vol Gls.	Agglut. Gls.	Opx	Pig	Mg-Cpx	Fe-Cpx
SiO₂	43.7	0.07	37.7	71.6	44.5 (39)	53.1	52.1	50.8	47.8
TiO₂	<0.04	52.6	0.08	0.39	0.92 (111)	0.68	0.60	1.10	1.39
Al₂O₃	35.0	0.10	<0.04	13.7	23.0 (80)	0.89	0.98	1.39	1.69
Cr₂O₃	0.05	0.39	0.14	0.07	0.21 (19)	0.42	0.44	0.49	0.17
MgO	0.07	2.83	37.1	0.56	7.69 (546)	25.2	20.9	14.5	6.53
CaO	19.3	0.22	0.13	1.24	14.1 (36)	1.71	4.63	19.0	13.3
FeO	0.15	42.1	24.0	0.71	7.26 (490)	16.8	19.1	11.2	27.9
Na₂O	0.50	<0.04	<0.04	1.19	0.41 (31)	<0.04	<0.04	0.07	0.05
K₂O	0.04	0.04	<0.04	7.51	0.15 (22)	<0.04	<0.04	<0.04	<0.04
Total	98.81	98.31	99.15	96.97	98.20	98.80	98.75	98.55	98.83

594
595

62231 -91 (10-20µm)									
	Plag	Ilm	Olivine	Vol Gls.	Agglut. Gls.	Opx	Pig	Mg-Cpx	Fe-Cpx
SiO₂	44.2	0.08	37.4	68.2	44.4 (37)	53.3	52.6	51.3	47.6
TiO₂	<0.04	52.7	0.09	0.20	0.91 (132)	0.59	0.74	1.17	1.36
Al₂O₃	34.8	0.06	<0.04	15.4	23.0 (76)	0.98	1.09	1.55	1.58
Cr₂O₃	<0.04	0.51	0.08	<0.04	0.18 (14)	0.39	0.41	0.46	0.13
MgO	0.06	3.24	35.2	0.16	7.66 (464)	24.2	21.9	14.8	6.09
CaO	19.2	0.33	0.17	1.52	14.2 (35)	1.69	4.43	18.2	13.8
FeO	0.11	41.2	26.5	1.37	7.34 (527)	18.0	18.1	11.6	28.0
Na₂O	0.53	<0.04	<0.04	1.11	0.45 (53)	<0.04	<0.04	0.08	0.04
K₂O	0.05	<0.04	<0.04	9.40	0.14 (29)	<0.04	<0.04	<0.04	<0.04
Total	98.95	98.12	99.44	97.36	98.29	99.15	99.27	99.16	98.60

596
597

Figure 1. Modal analyses of phases in the fine fractions of highland soils. These data are modified after those in a LPSC abstract [Taylor et al., 2003].

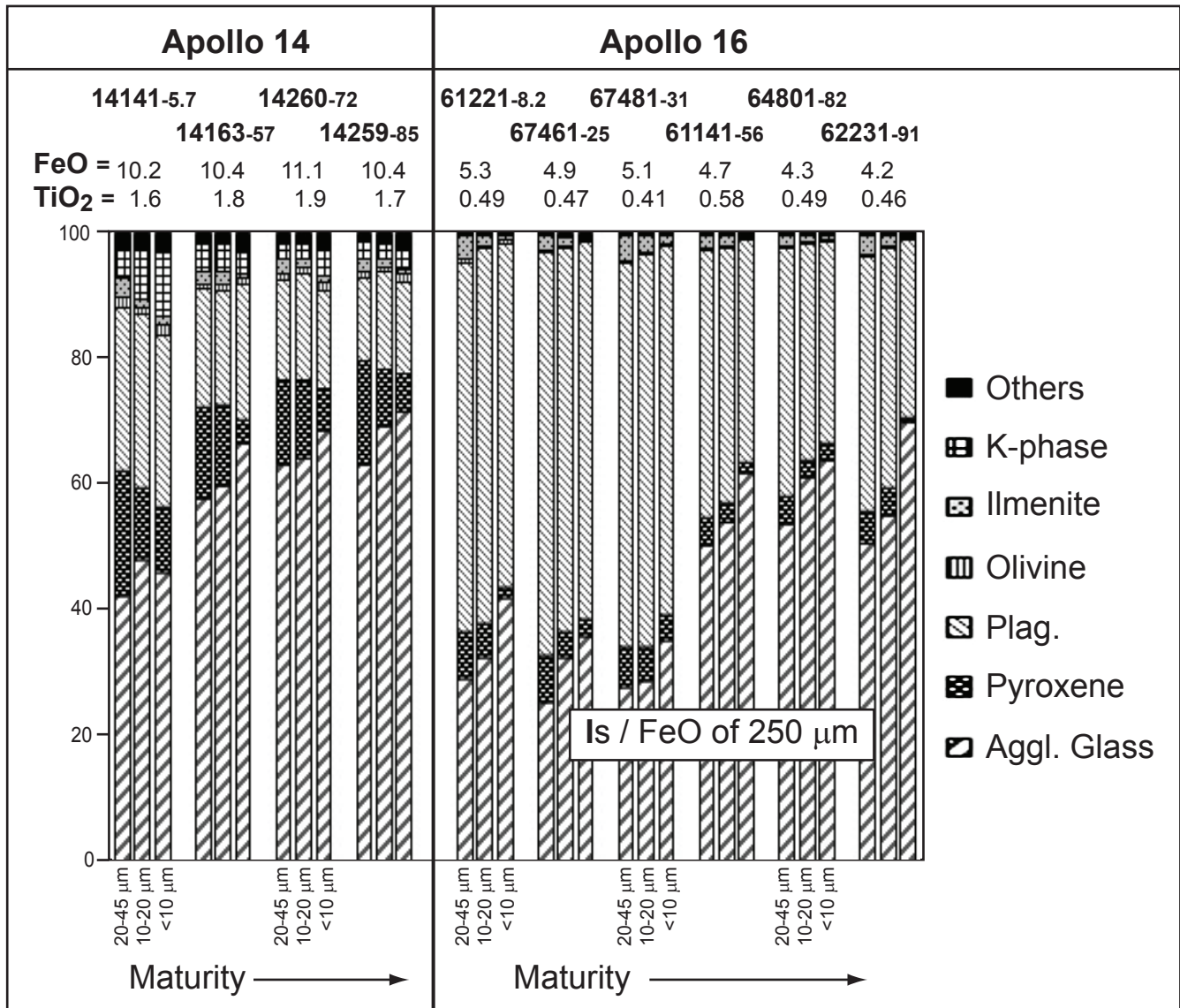


Figure 2. Comparisons of oxide components of the bulk chemistry of the fine fractions of high-land soils, in addition to their I_s/FeO values.

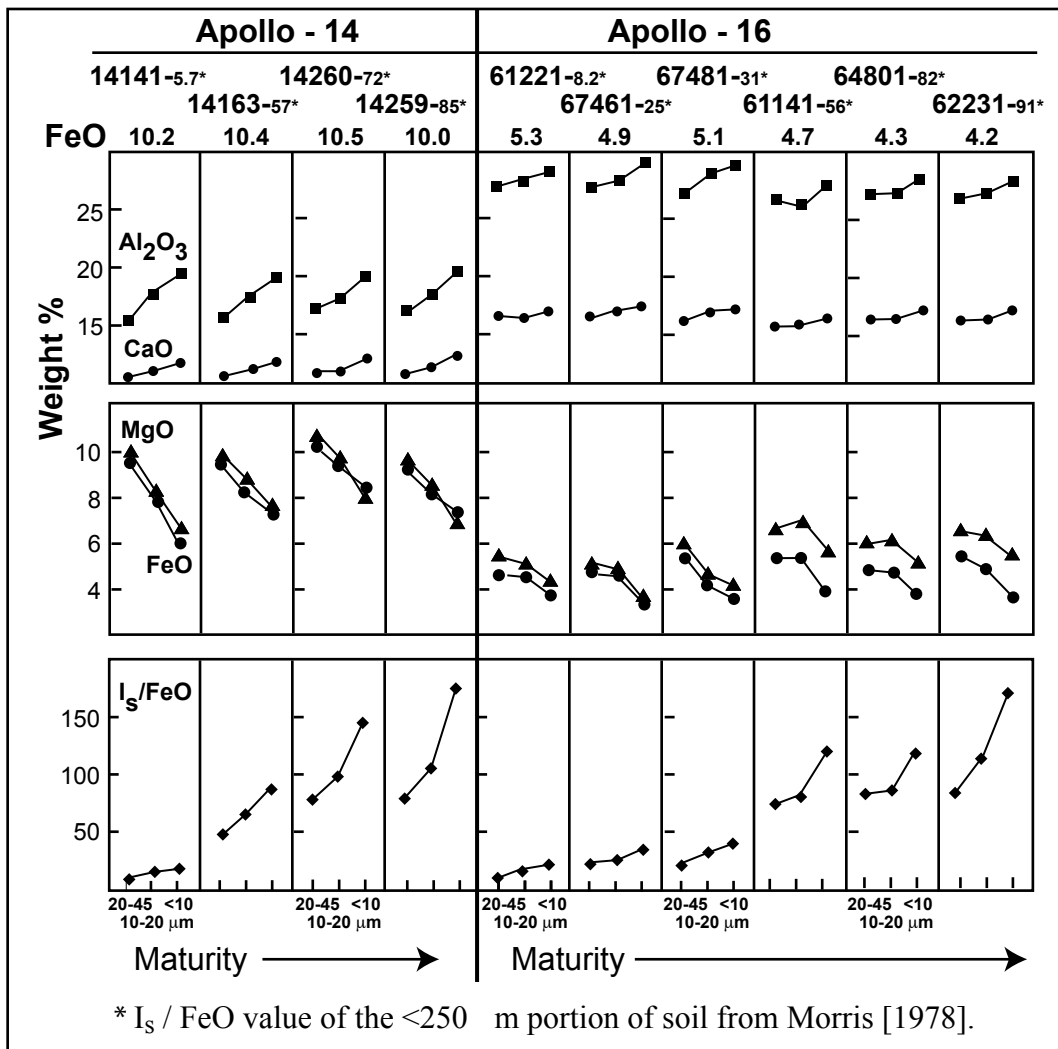


Figure 3. Comparison of chemistry of the agglutinitic glass with the bulk chemistry of the three soil size fractions for Apollo 16 highland soils. Modified from LPSC abstract [Taylor et al., 2003].

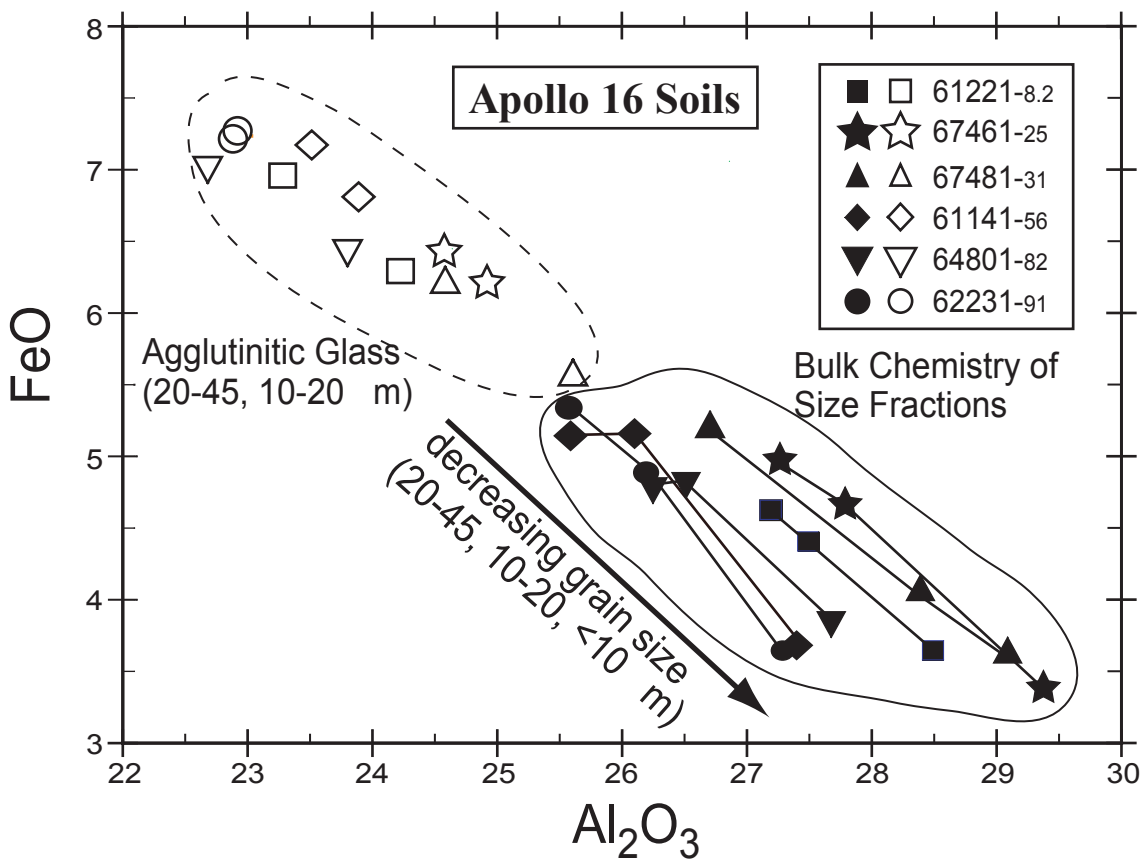


Figure 4. Chemistry of soil components relative to the chemistry of the bulk soil (<45 μm) for representative highland soils. The first three bars (blue shades) are the composition of three soil size separates (see legend). These are followed by the average composition of agglutinitic glass (red shades) present in the indicated size separate. The number in brackets is the I_S/FeO value for the bulk soil from Morris [1978]. Some of these data have been reported in Pieters and Taylor [2003a].

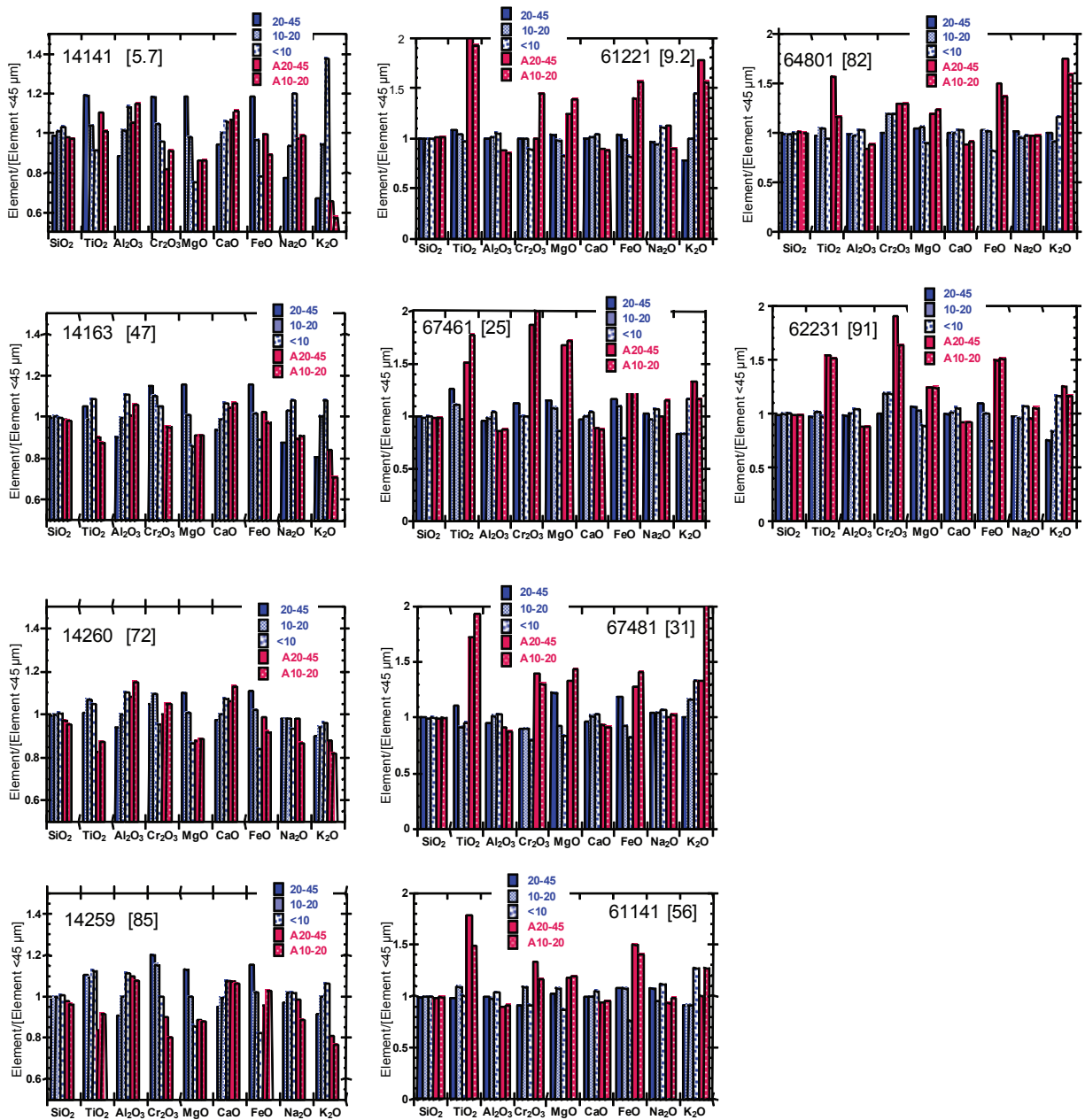


Figure 5. Bi-directional reflectance spectra of LSCC highland soils. Data for 64801 are from Pieters and Taylor [2003a].

